

3.3 A NEW INVERSION-BASED ALGORITHM FOR RETRIEVAL OF OVER-WATER RAIN RATE FROM SSM/I MULTICHANNEL IMAGERY

Grant W. Petty*
David R. Stettner

Purdue University
West Lafayette, Indiana

NAGW-2984
IN-47-CR
98154

1 INTRODUCTION

During the past few years, there has been a great deal of activity in the area of rainfall estimation from passive microwave sensors, in particular the Special Sensor Microwave/Imager (SSM/I). Most of the algorithms that have been published for this sensor are empirical or else are based on highly simplified physically derived relationships between single-scene microwave observables and rain rate. Representative examples include those described by Adler et al. (1993), Grody (1991), and others too numerous to list here.

Two published retrieval techniques take a far more detailed physical inversion approach; these include the algorithm described by Kummerow and Giglio (1994) and the Mugnai/Smith algorithm described by Mugnai et al. (1993) and references therein. These algorithms perform explicit forward radiative transfer calculations based on detailed model hydrometeor profiles and attempt to match the observations to the predicted brightness temperature.

The purpose of this paper is to discuss certain aspects of a new inversion-based algorithm for the retrieval of rain rate over the open ocean from SSM/I multichannel imagery. This algorithm takes a more detailed physical approach to the retrieval problem than the first class of algorithms mentioned above; at the same time, it avoids much of the complexity and computational burden of the Kummerow and Mugnai/Smith algorithms. Furthermore, despite the lack of prior empirical calibration, the prototype implementation performed respectably in two major algorithm intercomparison efforts — the NASA WetNet 1st Precipitation Intercomparison Project (PIP-1; Barrett et al. 1994) and the Global Precipitation Climatology Project (GPCP) 2nd Algorithm

Intercomparison Project (AIP-2). The main shortcoming noted was an apparent low bias of about a factor of 2.

The full details of the algorithm as originally implemented appear in a recent pair of papers by Petty (1994a,b). Details of its performance in the PIP-1 and AIP-2 intercomparisons may be found, respectively, in Barrett et al. (1994) and in a report scheduled for release by WCRP. The emphasis here will be on the impact of subsequent adjustments to the algorithm and on preliminary new validation results.

2 ALGORITHM

The principal distinguishing features of this algorithm relative to other published rain rate algorithms may be summarized as follows:

- The starting point for the inversion is not the raw brightness temperature fields from the SSM/I but rather normalized polarization differences P for 19.35, 37.0, and 85.5 GHz, coupled with an 85.5 GHz scattering index S_{85} . Petty (1994a) showed that the use of these single-frequency indices allows one to effectively separate radiative extinction (attenuation) due to precipitation from other geophysical variables (e.g., water vapor, surface wind speed, scattering by ice aloft) and, conversely, to reliably isolate the 85.5 GHz volume scattering signal from other sources of 85.5 GHz brightness temperature variability. Scattering and attenuation may thus be treated completely independently in the inversion algorithm, and background variability unrelated to the precipitation signal itself may be ignored.
- Observed rain cloud attenuation at 19 and 37 GHz serves as the primary basis for the rain rate retrieval, with 85.5 GHz scattering supplying information only in the event of heavy

*Corresponding Author Address: Grant W. Petty, Earth and Atmospheric Sciences Dept., West Lafayette, IN, 47907-1397

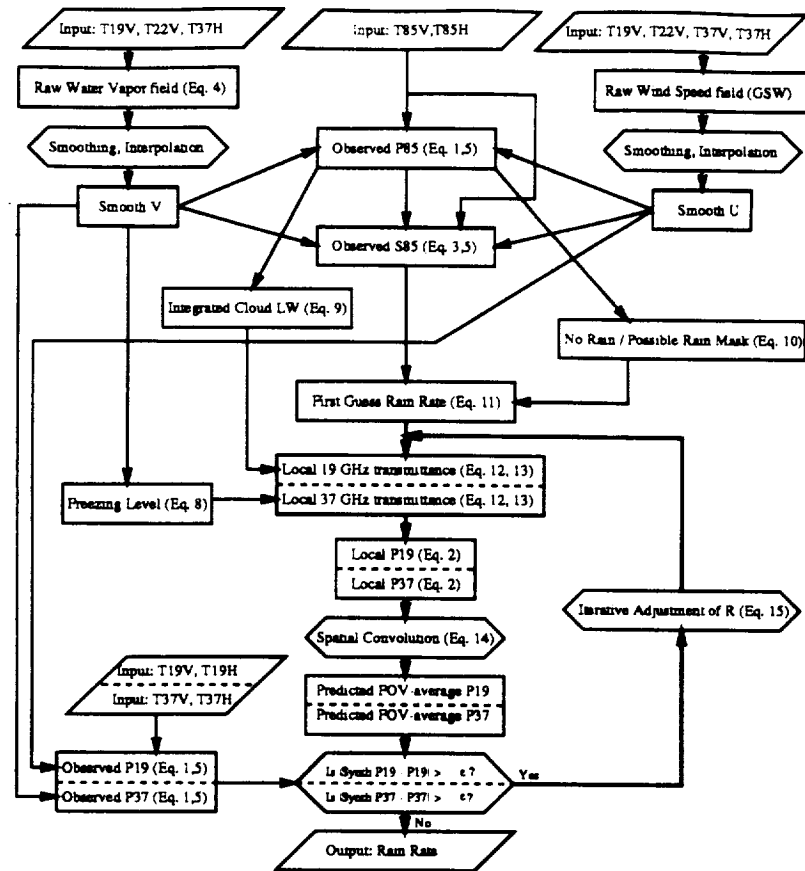


Fig. 1: Logical structure of the rain rate algorithm. Most indicated operations make use of spatial information in the SSM/I multichannel imagery (equation numbers refer to Petty 1994b).

rain exceeding the dynamic range of the 19 GHz channels.

- The inversion procedure entails an iterative adjustment of a 12.5 km resolution rain rate field in order to bring forward calculations of FOV-averaged normalized polarization at 19.35 and 37 GHz into approximate agreement with the corresponding observed fields. Because the forward calculation of normalized polarization involves only simple analytic functions of total cloud optical depth rather than full radiative transfer calculations, the algorithm is computationally efficient relative to other physical inversion methods. Also, this inversion strategy is unusual among current algorithms in its explicit treatment of footprint-filling effects.

3 CALIBRATION

Two aspects of recent calibration/validation efforts will be discussed here. The first is the classification of 12.5 km gridboxes as “no rain” or “possible rain”.

The second is the effect of minor adjustments in the scaling between observed scattering (S_{85}) and the first-guess rain rate field on algorithm biases relative to tropical atolls.

3.1 No Rain/Possible Rain Classification

One of the fundamental measures of the performance of any instantaneous rain rate retrieval algorithm is whether it correctly *delineates* the area of significant precipitation, irrespective of retrieved intensity. For the algorithm described here, the issue is particularly important, since the spatial distribution of “no rain” pixels strongly constrains the inversion in many cases. The classification is based on a threshold of the normalized 85.5 GHz polarization difference P_{85} , since this index is most sensitive to the presence of significant liquid water and allows areas of probable rain to be delineated with 12.5 km resolution. As published, an *ad hoc* threshold of $P_{85} < 0.413$ was employed based on the arbitrary assumption that FOV-averaged column liquid water amounts L in excess of 0.5 kg m^{-2} (corresponding to

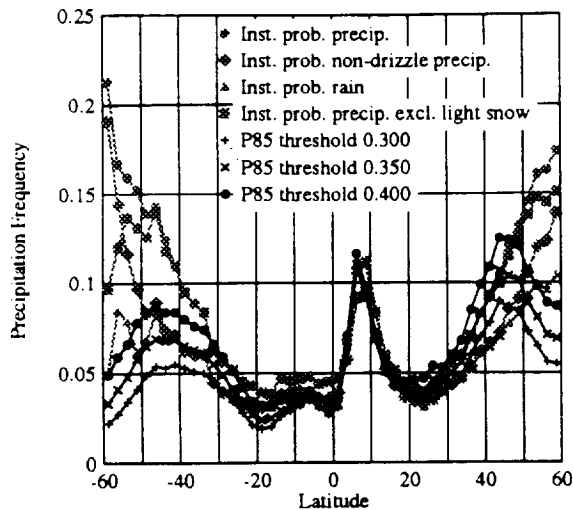


Fig. 2: COADS precipitation frequencies (gray lines) for 34 years compared with SSM/I P_{85} threshold-based frequencies for SON 1987.

$P_{85} \approx 0.213$) was likely to occur only in the presence of rainfall and that there was likely to be a random uncertainty of ~ 0.2 in the modeled relationship between P_{85} and L .

One aspect of the algorithm's performance which distinguished it from all others in PIP-1 was its retrieval of comparatively frequent precipitation at very high latitudes, especially south of 50°S . While there is little published information concerning expected climatological frequencies of over-ocean precipitation at those latitudes, the fact that most other participants in PIP-1 saw very little, if any, precipitation there was a cause for concern.

We therefore analyzed a 34 year record of ship-board present weather reports from the Comprehensive Ocean-Atmosphere Data Set (COADS) in order to derive a reasonable climatology of precipitation frequency over the global oceans. Fig. 2 depicts as gray lines the latitudinal dependence of precipitation frequency for various classes of precipitation. At latitudes between 40° and 60° (both hemispheres), precipitation is seen to be quite frequent, even when one excludes all forms other than actual rain.

Superimposed on those plots are solid black curves depicting the "possible rain" frequency inferred from three different P_{85} thresholds for SON 1987. Throughout the middle and low latitudes, the match between COADS precipitation frequencies and the occurrence of $P_{85} < 0.4$ is remarkably good. For reasons which are not yet understood, the P_{85} criterion appears to significantly overestimate the fre-

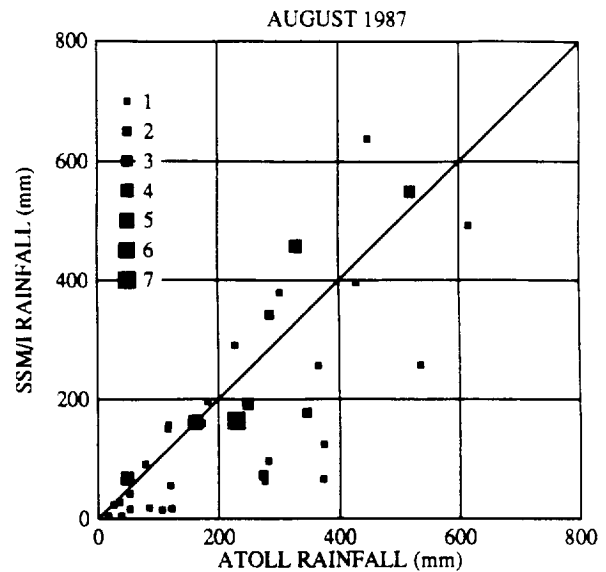


Fig. 3:

quency of rain (excluding drizzle and frozen precipitation) at approximately 45°N , while the agreement at far southern latitudes is excellent. Based on these results, we can find no basis for adjusting the P_{85} threshold employed in the "no rain"/"possible rain" determination.

3.2 Validation Against Tropical Atolls

A clear result of the PIP-1 exercise was that the first version of the algorithm underestimated tropical rainfall by about a factor of two. Even before this result was known, an unusually low scaling factor between 85.5 GHz scattering and the first-guess rain rate field was discarded in favor of one more in keeping with theoretical modeling results (see Petty 1994b for details). Since the first guess rain rate plays a particularly important role in regions of deep convection, the revised algorithm was used to recalculate monthly rain rate fields for August 1987 and the results compared with the tropical atoll data set of Morrissey et al. (1993). Atoll reports were divided up into non-overlapping groups falling within 2.5° boxes; the average of these groups was compared with the SSM/I estimate within that each box.

The size of the markers in Fig. 3 indicates the number of atolls contributing to the rainfall average within the respective grid box. In general, the agreement between satellite and atoll estimates is seen to improve dramatically as the number of atolls contributing to the 2.5° estimate increases.

Table 1: Statistical comparison between SSM/I (2.5 deg.) and tropical atoll monthly rainfall estimates for August 1987.

Min. Atolls	N	R_{atoll} (mm)	R_{sat} (mm)	Ratio	r
1	35	227.6	177.5	0.78	0.77
2	9	239.3	204.5	0.85	0.83
3	6	217.6	237.9	1.09	0.97

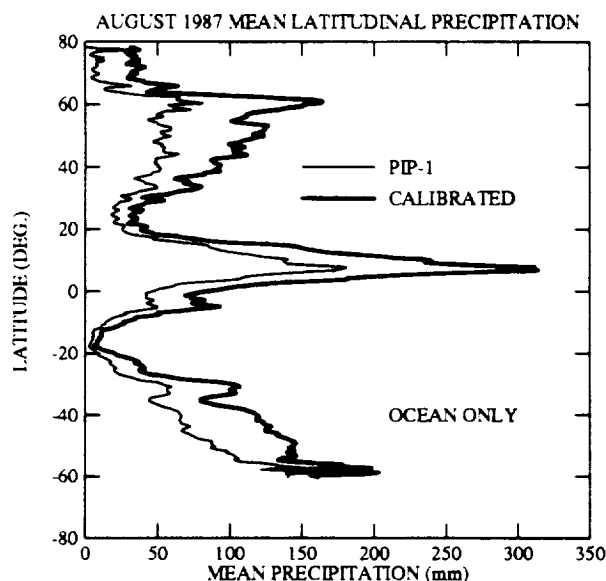


Fig. 4: Latitudinal oceanic rainfall for August 1987 from the uncalibrated algorithm submitted to PIP-1 and from the current version.

3.3 Latitudinal Averages

In order to assess the overall effect of various algorithm modifications, latitudinal averages of over-ocean rainfall were calculated for August 1987 and compared with results obtained with the prototype version of the algorithm submitted to PIP-1. The results appear in Fig. 4. The net result is a consistent increase by a factor of 1.5–2.0 of estimated rainfall, with somewhat larger increases over the far North Atlantic Ocean, and with somewhat smaller increases (as low as 20%) near 55°.

Given the absence of a significant bias relative to the tropical atolls, there is no reason to disbelieve the latitudinal averages found in the tropics. Rainfall estimates at high latitudes are certainly higher than those yielded by many other algorithms, but there is as yet little reliable basis for confirming or refuting any specific estimate in those data sparse regions. If one accepts the COADS rainfall fre-

quency of ~ 0.08 at 40–50°S, our algorithm's estimate of ~ 130 mm/month implies an average rainfall rate, conditioned on the occurrence of rain, of 0.17 mm hr^{-1} .

Acknowledgments

This work was supported by NASA Grants NAGW-2984 and NAG8-918.

REFERENCES

- Adler, R.F., A.J. Negri, P.R. Keehn, and I.M. Hakkarinen, 1993: Estimation of monthly rainfall over Japan and surrounding waters from a combination of low-orbit microwave and geosynchronous IR data. *J. Appl. Meteor.*, **32**, 335–356.
- Barrett, E.C., R.F. Adler, K. Arpe, P. Bauer, W. Berg, A. Chang, R. Ferraro, J. Ferriday, S. Goodman, Y. Hong, J. Janowiak, C. Kidd, D. Kniveton, M. Morrissey, W. Olson, G. Petty, B. Rudolf, A. Shibata, E. Smith, R. Spencer, 1994: The first WetNet Precipitation Intercomparison Project: Interpretation of results. Submitted to *Remote Sens. Rev.*
- Grody, N.C., 1991: Classification of snow cover and precipitation using the Special Sensor Microwave Imager. *J. Geophys. Res.*, **96**, 7423–7435.
- Kummerow, C.D., and L. Giglio 1994: A passive microwave technique for estimating rainfall and vertical structure information from space. Part I. Algorithm description. *J. Appl. Meteor.*, **33**, 3–18.
- Mugnai, A., E.A. Smith, and G.J. Tripoli, 1993: Foundations for physical-statistical precipitation retrieval from passive microwave satellite measurements. Part II: Emission source and generalized weighting function properties of a time dependent cloud-radiation model. *J. Appl. Meteor.*, **32**, 17–39.
- Petty, G.W., 1994a: Physical retrievals of over-ocean rain rate from multichannel microwave imagery. Part I: Theoretical characteristics of normalized polarization and scattering indices. To appear in *Meteorol. Atmos. Phys.*
- Petty, G.W., 1994b: Physical retrievals of over-ocean rain rate from multichannel microwave imagery. Part II: Algorithm implementation. To appear in *Meteorol. Atmos. Phys.*